



<https://doi.org/10.15407/ufm.23.01.027>

V.B. TARELNYK^{1,*}, O.P. GAPONOVA^{2,},
and Ye.V. KONOPLIANCHENKO¹**

¹ Sumy National Agrarian University,
160 Gerasym Kondratiev Str., UA-40021 Sumy, Ukraine

² Sumy State University,
2 Rymsky-Korsakov Str., UA-40007 Sumy, Ukraine

* tarelnyk@ukr.net, ** gaponova@pmtkm.sumdu.edu.ua

ELECTRIC-SPARK ALLOYING OF METAL SURFACES WITH GRAPHITE

The article reviews and analyses the current scientific research in the field of surface treatment of metal surfaces with concentrated energy fluxes (CEF) — the electric-spark (in the literature, known also as electrospark) alloying (ESA), which makes it possible to obtain surface structures with unique physical, mechanical and tribological properties at the nanoscale. The ESA method with a graphite electrode (electrospark carburizing — EC) is based on the process of diffusion (saturation of the surface layer of a part with carbon), and it is not accompanied by an increase in the size of the part. In this article, the influence of the EC parameters on the quality of the carburized layer is investigated. The microstructural analysis shows that the three characteristic zones could be distinguished in the structure: the carburized (“white”) layer, the finely dispersed transition zone with fine grain, and the base metal zone. The analysis of the results of the durometric studies of the coatings is carried out. To achieve the required parameters of dimensional accuracy and roughness of the working surface of the part after the EC process, it is necessary to use the method of non-abrasive ultrasonic finishing (NAUF). In addition, because of applying the NAUF method, the surface roughness is decreased, the tensile stresses are changed to the compressive ones, and the fatigue strength is increased too. In addition, to reduce the roughness of the treated surface, it is proposed to apply the EC technology in stages, reducing the energy of the spark discharge at each subsequent stage. In order to increase the quality of the carburized layer obtained by the EC process, it is proposed to use a graphite powder, which is applied to the treated surface before alloying. The comparative analysis shows that, after the traditional EC process at $W_p = 4.6$ J, the surface roughness of steel 20 is $R_a = 8.3\text{--}9.0$ μm , and after the proposed technology, $R_a = 3.2\text{--}4.8$ μm . In this case, the continuity of

Citation: V.B. Tarelnyk, O.P. Gaponova, and Ye.V. Konoplianchenko, Electric-Spark Alloying of Metal Surfaces with Graphite, *Progress in Physics of Metals*, **23**, No. 1: 27–58 (2022)

the alloyed layer increases up to 100%; there increases the depth of the diffusion zone of carbon up to 80 μm as well as the microhardness of the “white” layer and its thickness, which increase up to 9932 MPa and up to 230 μm , respectively. The local micro-x-ray spectral analysis of the obtained coatings shows that, at the EC process carried out in a traditional way, the applying $W_p = 0.9, 2.6, 4.6 \text{ J}$ provides the formation of the surface layers with high-carbon content depths of 70, 100, 120 μm , respectively, and with the use of a graphite powder, they are of 80, 120, 170 μm . While deepening, the amount of carbon is decreasing from 0.72–0.86% to the carbon content in the base metal — 0.17–0.24%. In the near-surface layer formed with the use of the new technology, the pores are filled with free graphite, which could be used as a solid lubricant to improve the operating characteristics of the friction-pairs parts processed thereby.

Keywords: electrospark (electric-spark) alloying, graphite, carburizing, microstructure, quality, wear resistance.

1. Problem Statement and Objective of the Study

Modern technology development is accompanied by an increase in operating modes of machines and mechanisms, which often operate at high speeds, loads and temperatures, as well as in the conditions of corrosive, abrasive and other types of working environments.

To protect the surfaces of parts from wear, they are subjected to various types of strengthening. These are: thermal spraying of protective cermet coatings [1–5], thermochemical treatment (TCT) [6–8], centrifugal reinforcement of steel surface layers with particles of tungsten carbide [9], electrochemical chromium coatings applied in flowing electrolyte [10], hard-facing with aluminium ceramics composition [11].

The development and implementation of effective technologies for surface strengthening is due, on the one hand, to the need to save expensive alloying elements, and, on the other hand, to the exaggeration of machine component parts operating conditions. One of the ways to solve this problem is to apply technologies that use concentrated energy fluxes (CEF) for processing materials, namely, plasma spraying [12–15], plasma treatment [16, 17], and laser processing [18–21]. Under non-equilibrium conditions of heating and cooling in the course of the CEF process, there occurs a formation of a surface layer having a fundamentally different structure in comparison with that obtained with the use of traditional thermal and mechanical methods.

Electrospark alloying (ESA), which makes it possible to obtain surface structures with unique physicomechanical and tribological properties at the nanoscale, is one of the modern methods of CEF processing metal surfaces [22].

Compared to the traditional technologies of surface strengthening, the ESA method has some advantages, as follows: locality, high degree of adhesion, appearance of low thermal background and, as a conse-

quence, the absence of warpage and deformation, ordinary and flexible technological process, environmental safety, *etc.* [23].

Despite the indisputable advantages of the method, it also has a number of disadvantages, such as a relatively small and uneven thickness of the formed layer, its porosity, roughness, *etc.* [24, 25].

The properties of the surface layers obtained by the contact and non-contact ESA methods in various media, on the different substrates, and with the use of the electrodes made of various conductive materials are described in [24–29].

When the electrodes approach to each other, the surfaces are subjected to the local actions of high impulse wave pressures and temperatures [30, 31]. In this case, instantaneously heating of the anode occurs, and a drop or solid particle of the anode material moves to the cathode. The fragments flying from the anode to the cathode are heated to a high temperature. The temperature of the short-duration heating of the surface microvolumes reaches $(5-7) \cdot 10^3$ K. The spark discharge occurs in the microscopically small volumes and is in progress for the period of 50 to 400 microseconds. On the cathode, there are formed dimples and micro baths, wherein the anode and cathode particles interact with each other and with the environment, while activating the diffusion processes and being resulted in the formation of new phases and the changes in the structures of the surface layers.

The available scientific groundwork in the field of using graphite in electric spark technologies is associated both with the study of phase changes in the surface layers of metals and alloys in the course of the ESA processes performed by graphite, and also with the improvement of the technologies for implementing these processes.

The wide possibilities for changing the properties of metal surfaces in the desired direction open up when using graphite as an anode in the ESA process. According to [32], the choice of graphite as an electrode material is conditioned by a number of its advantages. It is known that graphite in its free state is an excellent solid lubricant material, and in bound state, in the form of carbides, it is a solid wear-resistant phase, which is quite tolerant to many aggressive media [32, 33]. In some cases, a simultaneous combination of these properties is required.

The ESA method with a graphite electrode is based on the process of diffusion (saturation of the surface layer of a part with carbon), and it is not accompanied by an increase in the size of the part, which gives grounds to compare it with such a type of the thermochemical treatment (TCT) as an electrospark carburizing (EC) process [34–40].

With a carburizing process, strengthening the surface of a part occurs due to diffusion-hardening processes, which consist in local saturation the surface with carbon at a sufficiently high temperature (up to 10,000 °C), followed by rapid cooling to room temperature.

In Refs. [41–45], the authors investigated the EC process of steel surfaces, which has a number of advantages in comparison with the traditional ones carried out by the TCT methods. The main advantages of the EC processes are: achieving of 100% continuity for the strengthened surface; increasing the hardness of the surface layer of the part due to the diffusion-hardening processes; providing the possibility of local processing (alloying can be carried out in strictly specified places, without protecting the rest of the surface of the part), *etc.* With the EC processes, the discharge energies of 0.036 to 6.8 J and the productivities of 0.5 to 3.0 cm²/min are used.

When using the electrospark technologies, graphite is also applied to reduce the roughness of the surfaces, which have been preliminarily formed by the electrospark treatment with the other electrode materials (copper, silver, nickel, titanium) [46, 47]. It was shown that the most effective influence on the roughness of the coatings was exerted by the ESA process with graphite in the cases when the preliminary treatment had been carried out with the electrodes made of the metals not forming solutions with carbon, or of carbide.

The ESA process with graphite electrodes is also used to reduce the microhardness and increase the plasticity of the surfaces of nonferrous alloys, for example, the surface layer of beryllium bronze BrB2 [43, 48]. In this case, the time of alloying with carbon is determined by the required depth and microhardness of the surface layer.

In some cases, the ESA process with graphite electrodes is used as a preliminary treatment to prevent the seizure (sticking) of electrodes during subsequently processing and, thus, to increase the continuities of the coatings [43].

The ESA technology for processing metal surfaces with a graphite electrode and various technologies for reducing the roughness of steel samples after the electrospark carburizing process are used, when it is necessary, to increase the wear resistance and service life of the parts for the technological equipment and tools [49–51].

The results of the conducted research and the practical experience have shown the good perspectives for the development of this direction of the electrospark technology.

Thus, the accumulated data on the phase and structural transformations in the surface layers of steels and various metals during the ESA process by graphite, the information on the effects of the technological modes and machining work on the structure and properties of the carburized surfaces necessitate providing the analysis and systematization of literature and patent sources in this area.

The objective of this work is as follows:

- to study the influence of the parameters of the electrospark alloying process (discharge energy and alloying time) with a graphite electrode

on the quality (the coating roughness, microstructure, its continuity, phase composition and microhardness) of the carburized layer;

- to analyse the effects of the surface finishing methods, which are used after carburizing the surfaces, on the quality parameters of the obtained coatings;

- to investigate the effect of the discharge energy of the electro-spark alloying process by a graphite electrode with the use of graphite powder on the quality (roughness, microstructure of the coating, its continuity and microhardness) of the carburized layer;

- to specify the most rational modes for processing the carburized surfaces with using the method of the stepwise electrospark alloying process by graphite and also the method of non-abrasive ultrasonic finishing (NAUF) in order to reduce the roughness of the surface and optimize the properties thereof.

2. Evaluating the Quality Parameters of the Carburized Layer after Processing by the EC Method

In Refs. [41, 52–54], there were investigated the regularities, and there were obtained the quantitative data describing the effects of the processing time and the discharge energy (W_p) in the course of the ESA processing steel surfaces by graphite on the thickness, microhardness and roughness of the carburized layers. The samples of Armco-iron, steel of such grades as 20, 40X (40Kh), 38XM10A (38KhMYuA), 40XH2M10A (40KhN2MYuA), 30X13 (30Kh13), and 12X18H10T (12Kh18N10T) were used for the research. The ESA process was produced at the “EIL-8A (ЭИЛ-8А)” and “EIL-9 (ЭИЛ-9А)” units by the graphite electrodes in an automated mode at the range of discharge energies (W_p) of 0.6 to 6.8 J. The alloying productivity was equal to 1 and 5 min/cm².

The strengthening process was carried out at the screw-cutting lathe of 16K20 model. Vibrator 2 was attached to tool holder 4 through adap-

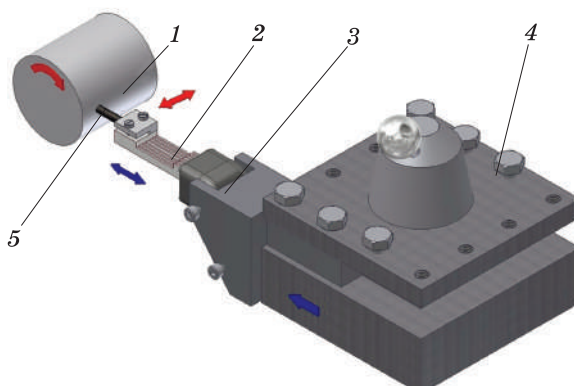


Fig. 1. Scheme of surface strengthening process in an automated mode: 1 — part; 2 — vibrator; 3 — adapter; 4 — tool holder; 5 — graphite electrode [54]

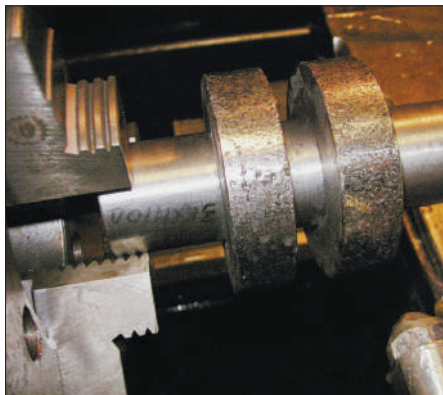


Fig. 2. Providing the NAUF process for a steel sample after electrospark carburizing thereof [41]

ter 3 (Fig. 1). Graphite electrode 5 was fed by the lathe mechanisms. The choice of the modes for automated strengthening (spindle rotation frequency, feed) was carried out because of the specified process productivity.

To implement the NAUF method, there were used the steel samples in the form of coils consisting of two disks having 50 mm in diameter and 10 mm wide. Those were connected by the intermediate rollers of 15 mm in diameter and had two technological sections of the same diameter to be fixed in the

course of processing. Before the EC process, the disk surfaces of the samples had been polished to $R_a = 0.5 \mu\text{m}$. Then the samples were fixed in the chuck of a lathe, and thereafter, the EC and NAUF processes were performed using the ПМС-39 (PMS-39) magnetostrictive transducer and the УЗУ-030 (UZU-030) ultrasonic generator (Fig. 2).

The main parameters for assessing the quality of the surface layer after the EC process were the thickness of the carburized layer, its structure and microhardness, as well as the surface roughness. Simultaneously, the structure and hardness of the base material (the substrate material) were analysed. The results of the analyses have shown that with an increase in the processing time and discharge energy, the thick-

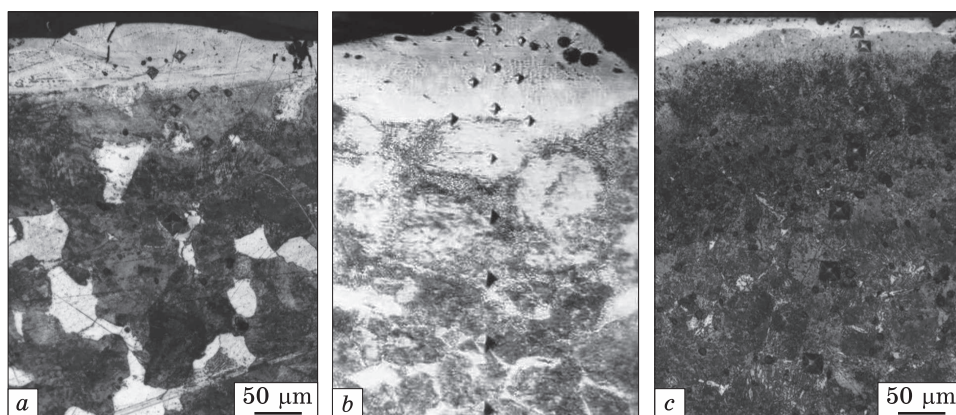


Fig. 3. Cross-sectional view of samples made of steel 38XM10A (38KhMYuA) (a) and 40XH2M10A (40KhN2MYUA) (b, c) after the EC process. Processing time (productivity) — 1 min/cm²: a — $W_p = 0.9 \text{ J}$ ($\times 200$); b — $W_p = 0.60 \text{ J}$ ($\times 200$); c — $W_p = 2.83 \text{ J}$ ($\times 250$) [41]

Fig. 4. Distribution of hardness HV in the carburized layer of steels 38XMIOA (38KhMYuA) (1) and 40XH2MIOA (40KhN2-MyuA) (2) after the EC process ($W_p = 0.9 \text{ J} - 5 \text{ min/cm}^2$), 40X (40Kh) after the stage carburizing process ($W_p = 2.83$ and $0.9 \text{ J} - 5$ and 2 min/cm^2 , respectively) and the NAUF process treatment (3) [41]

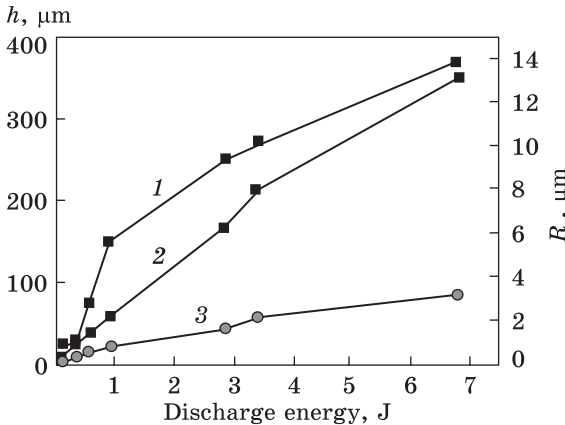
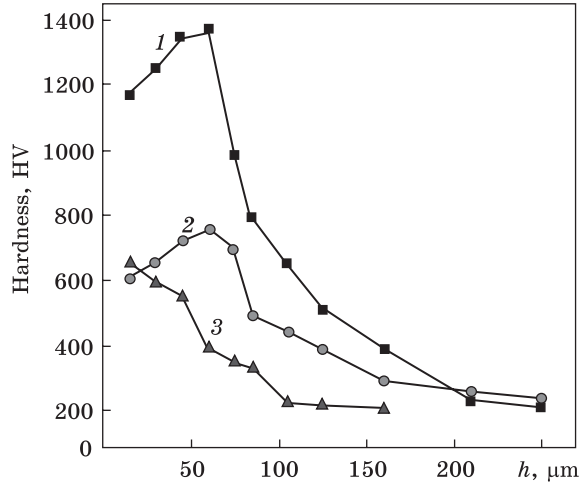


Fig. 5. The discharge energy dependent thickness of the carburized layer h (1) and surface roughness R_a (2) after the EC process, and after the EC as well as NAUF processes (3) of 38XMIOA (38KhMYuA) steel [41]

ness of the carburized layers increases, and the structure of the base material remains unchanged (Fig. 3).

The three characteristic zones can be distinguished in the structures of the samples: the carburized (“white”) layer, the finely dispersed transition zone with fine grain, and the base metal zone. The closer to the surface, the higher the microhardness in the subsurface layer is available.

The Vickers hardness on the surface is 1350 and 760 HV for 38XMIOA (38KhMYuA) and 40XH2MIOA (40KhN2MyuA) steels, respectively (Fig. 4). As it deepens, the hardness decreases and smoothly transforms into the hardness of the base, respectively, 225 and 250 HV (Fig. 4). The decrease in the hardness on the surface of the carburized specimens is associated with the heterogeneous structures of the hardened layers, the presence of the thin troostite (dispersed mixtures of ferrite and cementite) strips or meshes on the surfaces. The thicknesses of the troostite strips are of 50 to 60 μm . As a rule, there are no such

Table 1. The quality parameters for the surface layers of the samples [54]

Discharge energy W_p, J	Alloying time, min	Layer total depth, μm	Microhardness, HV	Roughness R_a , μm
Armco-iron				
0.6	1	35	950	0.8–0.9
1.41		100	900	1.0–1.6
2.83		144	840	5.5–6.3
3.4		153	870	8.3–8.5
6.8		180	900	—
0.6	5	37	985	—
1.41		163	970	1.2–1.6
2.83		245	1002	5.7–6.7
3.4		262	1006	8.6–8.9
6.8		310	1070	11.9–14.1
Steel 12X18H10T (12Kh18N10T)				
0.6	1	30	950	0.8–0.9
1.41		71	900	1.0–1.8
2.83		96	840	5.1–6.7
3.4		101	870	8.3–9.0
6.8		115	900	11.0–14.2
0.6	5	48	1013	0.9–1.0
1.41		134	1101	1.0–1.7
2.83		200	974	5.8–6.7
3.4		210	960	8.2–8.8
6.8		250	1100	11.0–14.5
Steel 30X13 (30Kh13)				
0.6	1	34	1050	0.7–0.9
1.41		134	978	1.1–1.7
2.83		196	909	5.8–6.3
3.4		209	1072	8.0–8.5
6.8		245	1027	11.9–14
0.6	5	48	1020	0.8–1.0
1.41		358	1005	1.2–1.7
2.83		623	1100	5.9–6.7
3.4		684	993	8.7–8.8
6.8		860	1000	11.9–14.1
Steel 40X (40Kh)				
0.6	1	35	950	0.7–1.1
1.41		146	900	1.2–2.3
2.83		215	980	5.5–6.8
3.4		230	960	8.3–9.1
6.8		270	1010	11.5–15
0.6	5	50	987	0.8–0.9
1.41		377	993	1.5–2.7
2.83		658	1001	5.6–6.5

strips after the NAUF process. The experiments have shown that with EC processing of steel 20, there is no troostite strip.

It has been set that while carburizing the steel surfaces by electro-spark alloying, with an increase in the discharge energy and alloying time, not only the thickness of the hardened layer increases, but also the surface roughness does (Fig. 5). The Vickers hardness on the surface for 38XM10A (38KhMYuA) steel varies within of 1200 to 1400 *HV*.

Table 1 shows the values of the total depths of the strengthened layers, as well as the values of microhardness and roughness of the surface layers of the samples after the EC process for 1 and 5 min.

As it can be seen from Table 1, with an increase in the discharge energy and alloying time (productivity) for all substrate materials, the depth of the strengthened layer, the microhardness, and the roughness of the surface layer increase.

2.1. Phase Composition of Surface Layer after the EC Process

As found [55], the ESA processing of iron alloys by graphite forms a strengthened layer that combines ductile austenite and hard carbide. High cooling rates lead to the creation of phase compositions according to metastable diagrams with the formation of carbides and other metastable phases. In this case, graphite in its free form does not plate out. When using compact metal electrodes and powders of graphite, ferrosilicon, or copper, in the formed layer, it is possible to obtain the free graphite, which is used as a solid lubricant to improve the performance characteristics of friction pair parts made of steel, titanium and copper alloys [33]. The studies of the phase formation mechanism during the electrospark carburization process [56] showed that the formation of the cementite phase (Fe_3C) in the surface layer of the steel samples occurred passing the stages of the formation of the liquid phase, its saturation with carbon and nitrogen ions, followed by the rapid crystallization with the formation of the residual austenite and iron nitride (Fe_4N). To increase the wear and corrosion resistance of the copper parts in a number of chemical media, they were treated with the use of the ESA method first by the aluminium and then graphite electrodes [57]. In Refs. [54, 58], to determine the phase composition of the formed strengthened layer, the method of x-ray structure analysis was used.

X-ray phase analysis of the samples was carried out at the unit of ДРОН-3М (DRON-3M) type in cobalt (CoK_α) monochromatic radiation. The tube operating modes were $U = 45$ kV, $I = 40$ mA. The lines (of the intensity of the reflected rays) were recorded on the diagrammatic tape of the ЖКС-4 (LKS-4) recorder. The tape movement speed was 1800 mm/h. The phases were identified by comparing the experimentally obtained interplanar spacings with the tabulated or theoretical distances for those phases that might be present in the samples.

There were analysed the samples of steels 40X (40Kh), 30X13 (30Kh13), and 12X18H10T (12Kh18N10T) after EC processing them in different energy modes. The research results are shown in Table 2.

The analysis of the research results showed as follows below.

- Because of strengthening of the 40X (40Kh) steel samples, the γ -Fe phase (25%) and the iron carbide (Fe_3C) phase (63%) are formed, which fact provides for increasing the microhardness of the surface layer.

- While analysing the samples made of steel 30X13 (30Kh13), it was found that the formations of γ -Fe, as well as iron and chromium carbides, respectively, Fe_3C and Cr_{23}C_6 , were observed, and the formation of carbides directly depended on the energy mode of processing, namely, the higher the mode, the greater the percentage of carbide formation in the total phase composition of the surface strengthened layer was available.

- When analysing the samples of steel 12X18H10T (12Kh18N10T), it was found that the following phases were formed: α -Fe, γ -Fe and X-phase. The X-phase was understood as a phase having an indefinite structural formula.

Table 2. Phase composition of the surface layer of the samples before and after EC processing [54]

Base material	Discharge energy, J	Processing time of 1 cm ² , min	Phase composition				
			α -Fe, %	X, %	γ -Fe, %	Fe_3C , %	Cr_{23}C_6 , %
Without processing							
Steel 40X(40Kh)	—	—	≈100	—	—	—	Traces
Steel 30X13(30Kh13)	—	—	≈100	—	—	—	Traces
Steel 12X18H10T (12Kh18N10T)	—	—	1	—	99	—	—
After EC processing							
Steel 40X(40Kh)	1.4	5	12	—	25	63	—
Steel 30X13(30Kh13)	0.5	10	16	—	6	78	—
Steel 12X18H10T (12Kh18N10T)	1.4	1	10	68	22	—	—
Steel 12X18H10T (12Kh18N10T)	6.8	1	15	43	42	—	—
Steel 12X18H10T (12Kh18N10T)	6.8	5	16	52	32	—	—

2.2. Applying the Methods for Finishing the Surfaces after the EC Process to Increase the Quality of Coatings

To achieve the required parameters of dimensional accuracy and roughness of the working surfaces of the parts after the EC process, it is necessary to use additional processing methods. Such methods can be, for example, the grinding with abrasive wheels, and the methods of surface plastic deformation such as ball rolling, diamond burnishing, *etc.*

According to [59, 60], the ball rolling operation allows reducing the surface roughness and eliminating the residual tensile stresses. After such processing of the electric-spark coatings, the macrostresses become compressive, and their values little depend on the rolling forces.

The diamond burnishing operation, unlike the ball rolling one, allows processing parts having rather high hardness [61]. The use of a spherical diamond as a tool allows providing local plastic deformation with reducing surface roughness, waviness, and porosity [62].

Recently, the NAUF process has found wide application [63]. This method is based on the fact that in the course of processing, between the deforming element and the surface to be treated, there is occurred a periodic contact with the frequency of ultrasonic vibrations. At the moment of contact, the instantaneous stresses are significantly higher than the average ones, which results in significant plastic deformations. Same as for other methods of surface deformation, because of the NAUF operation, the surface roughness decreases. Experience has shown that with the NAUF process, the tensile stresses in the surface layer occurred in the course of the ESA process change into the compressive ones, which arise while processing [64]. According to [54], at strengthening the surfaces by performing the EC process followed by the NAUF operation, an increase in fatigue strength is observed by 1.2 times as compared to the sample without strengthening (645 instead 543 MPa) and by 1.57 times as compared to the sample after the EC process (645 instead 410 MPa).

In Ref. [65], according to the results of the experimental studies of the influence of the methods of surface plastic deformation on the microgeometry, structure, and properties of the ESA layers, it has been revealed that the efficiency of surface plastic deformation as a method for reducing surface roughness depends on the specific rolling force and the type of the ESA method; the dependences of the microhardness of the surface layers on the specific deformation force have been found; it has been disclosed that the most rational modes of the specific forces of the surface plastic deformation methods for coatings made of hard wear resistant materials are 1000 and 1500 MPa, respectively, for the diamond burnishing operation and the one of ball rolling.

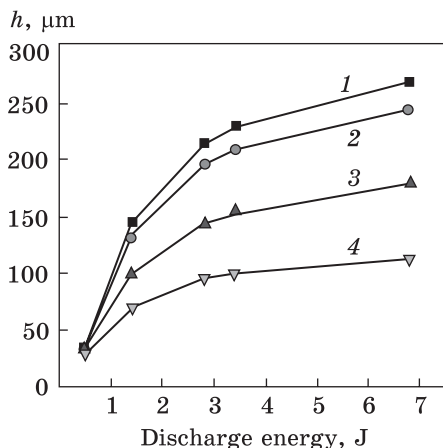


Fig. 6. The dependence of the carbonized layer thickness h on the discharge energy after EC processing of the surfaces of steels 40X (40Kh) (1), 30X13 (30Kh13) (2), Armco-iron (3) and steel 12X18H10T (12Kh18N10T) (4) [41]

The results of the investigations of the total thickness of the layer of increased hardness, the maximum microhardness on the surface and the roughness after the EC and the NAUF processes and also after grinding of steels 40X (40Kh)

and 12X18H10T (12Kh18N10T) are given in Table 3. The duration time of the electrospark alloying process with a graphite electrode was 5 min/cm².

The experimental results have shown that the depth of the carbonized layer and its microhardness in the same technological conditions significantly differ for different steel grades. Fig. 6 shows the results of measuring the depths of the strengthened layers of the substrates

Table 3. Quality parameters of the surface layers of the samples made of steels 40X (40Kh) and 12X18H10T (12Kh18N10T) after the EC, NAUF and the grinding processes [54]

Discharge energy, J	Sample processing method	Layer depth, μm		Microhardness, HV		Roughness R_a , μm	
		40X (40Kh)	12X18H10T (12Kh18N10T)	40X (40Kh)	12X18H10T (12Kh18N10T)	40X (40Kh)	12X18H10T (12Kh18N10T)
0.6	EC + NAUF	50	50	980	880	0.2	0.2
	EC + NAUF + grinding	40	48	920	841	0.6	0.6
	EC + grinding	10	18	780	723	0.6	0.6
	EC	50	48	987	1013	0.9	0.9
2.83	EC + NAUF	657	210	920	970	0.8	0.8
	EC + NAUF + grinding	635	195	895	950	0.8	0.8
	EC + grinding	580	130	770	790	0.8	0.8
	EC	658	200	1000	974	5.6	5.8
6.8	EC + NAUF	908	244	854	985	0.8	0.8
	EC + NAUF + grinding	895	220	840	875	0.8	0.8
	EC + grinding	856	110	824	670	0.8	0.8
	EC	910	250	1050	1100	11.9	14.5

made of Armco-iron and a number of steels, which had been obtained with EC processing by 1 min/cm² at different values of the discharge energy. The data in Table 3 and Fig. 6 differ, since it takes different periods of time for EC processing of one cm² for the different sample surfaces (5 and 1 min/cm², respectively).

The experiments have shown that there is a clear relationship between the depth of EC processing and the carbon content in the steel. The EC depth is greater, the larger the carbon content of the steel is. The depth of carburizing for 40X (40Kh) steel having an average carbon content close to 0.4% in the initial state is significantly greater than that of Armco iron and 12X18H10T (12Kh18N10T) steel containing up to 0.12% of carbon. The more W_p value, the more significant this difference is. The curve of the dependence of the carburization depth on W_p for steel 30X13 (30Kh13) (carbon content is of 0.26 to 0.35%) occupies an intermediate position. At EC processing the steels of 40X (40Kh) and 12X18H10T (12Kh18N10T) grades with the productivity of 5 min/cm² and $W_p = 6.8$ J, the difference in the thicknesses of the strengthened layers reaches 660 μm (Table 3).

2.3. Stepwise EC Processing

According to [66], the main parameters of the surface layer quality include as follows: roughness, structure, microhardness, and residual stresses. Despite the fact that the NAUF treatment of the steel surfaces after ESA processing with the use of a graphite electrode significantly reduces the roughness, for a lot of the machine parts this is insufficient. A grinding procedure cannot be applied after EC processing, since in this case, at least 50–100 microns of the surface layer having the highest hardness is removed. It is reported that to reduce the roughness of the electric-spark coating, it is sufficient to carry out so called “soft” alloying with graphite as a final operation. Burnishing occurs both due to heating and softening of the scallops under the action of a red-hot graphite electrode, as well as ejection of the cathode metal and destruction of protruding parts of the surface at the places where the pulses are applied [46, 67]. The experience has shown that “soft” alloying by graphite sometimes does not sufficiently reduce the surface roughness. In Refs. [38, 68], the ESA technology is recommended to be applied to surfaces after EC processing with the same graphite electrode, but step by step, while at each subsequent stage, the spark discharge energy should be reduced. At each successive stage, the ESA process is performed by a graphite electrode using such a discharge energy at which a surface having a roughness of 2 to 3 times lower than at the previous stage was formed. The alloying time was empirically determined, and, depending on the value of W_p , varied in the range of 0.5 to 2.0 min/cm² (Table 1).

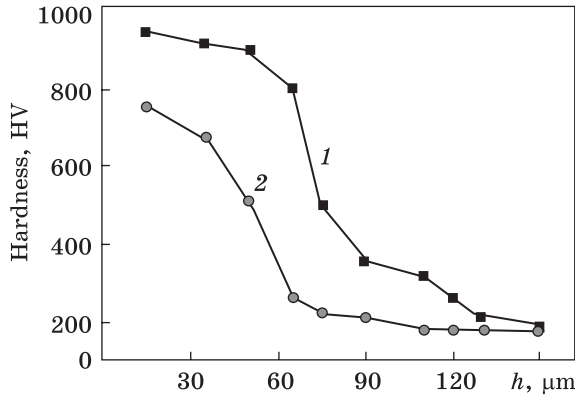


Fig. 7. The distribution of Vickers hardness HV over the depth of the carburized layer of steel 20 after the EC treatment at $W_p = 2.83$ J (1) and after the stepwise EC treatment at $W_p = 2.83, 0.9, \text{ and } 0.1$ J (2) [41]

Table 4. The results of reducing the surface roughness of the steel samples after EC processing [54]

Steel grade	Dis-charge energy, W_p , J	Roughness R_a , μm						
		After EC	Productivity, T , min/cm^2					
			Discharge energy, W_p , J					
			0.1	0.31	0.53	0.9	2.83	3.4
38XMFOA (38KhMYuA)	0.1	0.8–0.9						
	0.31	0.9–1.0	$\frac{0.8-0.9}{2}$					
	0.53	1.4–1.7	$\frac{0.8-0.9}{2}$	$\frac{0.9-1.0}{1}$				
	0.9	1.7–2.1	$\frac{0.9-1.0}{2}$	$\frac{1.0-1.1}{1}$	$\frac{1.4-1.7}{1}$			
	2.83	5.7–6.9	$\frac{1.1-1.2}{14}$	$\frac{1.2-1.3}{6}$	$\frac{1.6-1.9}{3}$	$\frac{1.7-2.2}{2}$		
	3.4	8.3–8.9	$\frac{1.3-1.6}{18}$	$\frac{1.4-1.7}{7}$	$\frac{2.0-2.3}{4}$	$\frac{2.3-2.7}{3}$	$\frac{5.7-6.7}{0.5}$	
	6.8	11.9–14	$\frac{1.6-1.9}{25}$	$\frac{1.8-2.1}{13}$	$\frac{2.4-2.6}{8}$	$\frac{2.6-3.1}{5}$	$\frac{6.3-6.9}{0.5}$	$\frac{8.5-9.0}{0.5}$
40XH2MFOA (40KhN2MyuA)	2.83	5.7–6.7	$\frac{1.0-1.1}{14}$	$\frac{1.2-1.3}{6}$	$\frac{1.5-1.8}{3}$	$\frac{1.7-2.1}{2}$		
12X18H10T (12Kh18N10T)	2.83	2.9–3.7	$\frac{0.8-0.9}{14}$	$\frac{1.0-1.2}{6}$	$\frac{1.5-1.8}{3}$	$\frac{1.7-2.0}{2}$		

An increase in the alloying time does not contribute to a decrease in the value of the surface roughness.

Table 4 shows the results of the effects of stepwise EC processing on the roughness of the samples. So, for example, after the EC treatment of 38XMFOA (38KhMYuA) steel at $W_p = 2.83$ J, the surface roughness is $R_a =$ of 5.7 to 6.9 μm . After the EC treatment with the $T = 2$ min/cm^2 and $W_p = 0.9$ J, the surface roughness is $R_a =$ of 1.7 to 2.2 μm . Subsequent step-by-step alloying can provide for obtaining $R_a =$ of 1.1 to 1.2 μm .

According to [38], in order to reduce maximally the surface roughness, for example, of steel 38XM10A (38KhMYuA), which, after EC processing at $W_p = 6.8$ J, is $R_a = 11.9\text{--}14.0$ μm , it is necessary:

- during the first stage, to perform the EC treatment at $W_p = 2.83$ J, *i.e.* with W_p , providing a ≈ 2 fold decrease in the roughness value (from $11.9\text{--}14.0$ to $6.3\text{--}6.9$ μm); The ESA productivity (T) is 0.5 min/cm^2 ;
- during the second stage, to perform the EC treatment at $W_p = 0.9$ J, *i.e.*, with W_p , providing a ≈ 3 fold decrease in the roughness value (from $6.3\text{--}6.9$ to $1.7\text{--}2.1$ μm); the ESA productivity (T) is 2 min/cm^2 ;
- during the third stage, to perform the EC treatment at $W_p = 0.1$ J, *i.e.* with W_p , providing a ≈ 2 fold decrease in the roughness value (from $1.7\text{--}2.1$ to $0.8\text{--}0.9$ μm); the ESA productivity (T) is 2 min/cm^2 ;

It should be noted that EC processing in any mode does not allow achieving similar results.

Analysing the distribution of the microhardness in the samples made of steel 20 after the EC treatment at $W_p = 2.83$ J and the stepwise EC treatment at $W_p = 2.83, 0.9$, and 0.1 J (Fig. 7), it can be noted that in both cases, the highest microhardness of the strengthened layer is observed closer to the surface. For the first sample, it is of 920 to 950 HV and the depth thereof is up to 60 μm , and for the second sample, it is of 690 to 720 HV at the depth of 30 μm . With increasing the distance from the surface for both samples, the values of microhardness gradually decrease, and at the depths of 130 and 100 μm , they correspond to the microhardness of the base material, namely, 180 HV . Decreasing the thickness and microhardness of the strengthened layer for the sample processed with the use of a stepwise EC treatment can be explained both by the influence of the impact action of a graphite electrode heated to a high temperature and by a slight erosion of the substrate. Earlier, it had been shown [69] that a mechanical shock action on the carburized layer resulted in grinding of carbides and redistributing of carbon in the surface layer of 30 to 40 μm thick.

Thus, as a result of the stepwise EC treatment of steel 20, the following parameters are changed: the surface roughness of the layer is reduced from $R_a = 4.79$ to $R_a = 1.10$ μm and from $R_z = 13.62$ to $R_z = 3.14$ μm ; the microhardness of the “white” layer is lowered from $920\text{--}950$ HV to $690\text{--}720$ HV ; the depth of the zone of increased hardness is decreased from 130 to 100 μm .

2.4. EC Processing by a Compact Electrode Using Graphite Powder

Despite the advantages inherent for stepwise EC processing, this method has a number of disadvantages, namely, a decrease in the microhardness and thickness of the strengthened surface layer, and relatively long duration of the process for reducing the roughness.

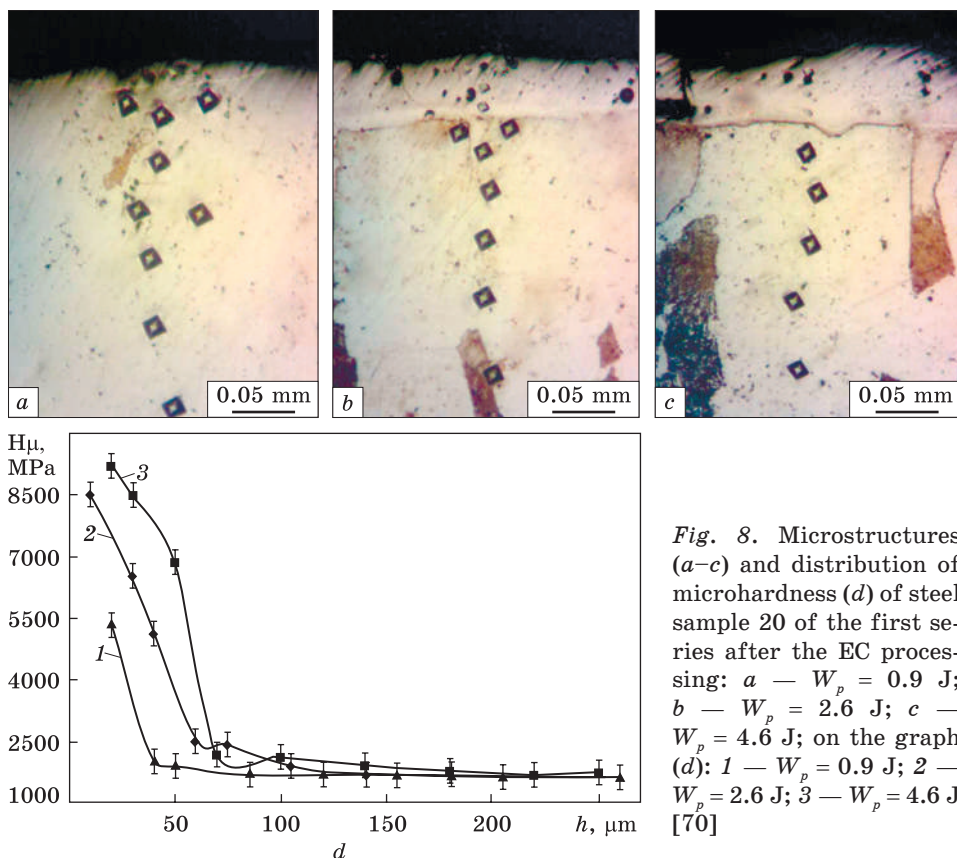


Fig. 8. Microstructures (a-c) and distribution of microhardness (d) of steel sample 20 of the first series after the EC processing: a — $W_p = 0.9$ J; b — $W_p = 2.6$ J; c — $W_p = 4.6$ J; on the graph (d): 1 — $W_p = 0.9$ J; 2 — $W_p = 2.6$ J; 3 — $W_p = 4.6$ J [70]

In Ref. [70], the aim of the paper was to improve the quality of the steel part surface layers (reducing roughness, increasing the thickness of the carburized layer, microhardness and continuity thereof) by improving the process of carburization with the use of the ESA method, due to the combined use of a compact graphite tool electrode and a graphite powder during the alloying process.

For the research, the two series of the samples made of steels 20 and 40X (40Kh) were used.

In the first series, the samples were processed using the traditional technology, namely, in one mode and with the same productivity at the EC treatment by a compact tool electrode.

In the second series, the samples were processed stepwise.

At the first stage, the EC treatment of the sample surface was carried out in accordance with the specified discharge energy and with the productivity of 1 min/cm².

At the second stage, on the part surface formed at the first stage, carefully rubbing, the graphite powder in the form of a suspension

made in a ratio of $\approx 80\%$ graphite powder and 20% petroleum jelly was applied.

At the third stage, not waiting for drying the above said suspension, EC processing was carried out on the surface having been treated at the second stage, and in the same mode and with the same productivity as at the first stage.

The distribution of the elements (carbon and iron) in the surface layer was determined on a scanning electron microscope of SEO-SEM Inspect S50-B type equipped by Aztec One Energy-Dispersive Spectrometer with X-MaxN20 Detector (manufactured by Oxford Instruments plc).

In Fig. 8, there are shown the microstructures (*a-c*) and the distribution of the microhardness over the layer thickness (*d*) of the samples made of steel 20 for the first series after EC processing with the use of $W_p = 0.9, 2.6, \text{ and } 4.6 \text{ J}$. The results are summarized in Table 5.

The metallographic analysis showed that the microstructures after EC processing consist of 3 zones: the upper so-called “white” layer, which is not etched in a reagent, the diffusion zone, and the base having a ferritic-pearlitic structure corresponding to steel 20. It should be noted that with increasing discharge energy, the values of thickness and continuity of the “white” layer increase (Table 5).

The results of the durometric studies indicate that the maximum microhardness (8492 MPa) is determined on the samples after EC processing performed at a discharge energy $W_p = 4.6 \text{ J}$.

While comparing the influence of the traditional and proposed EC technologies on the qualitative parameters of the surface layer, it should be noted that after processing the surface with the use of the proposed EC technology, the surface roughness decreases. Thus, after traditional EC processing at $W_p = 4.6 \text{ J}$, the surface roughness is $R_a = 8.3\text{--}9.0 \text{ }\mu\text{m}$, and after the proposed one, its roughness is $R_a = 3.2\text{--}4.8 \text{ }\mu\text{m}$.

Table 5. Summary Table of surface quality parameters for samples of steel 20 after the EC processing [70]

Discharge energy, W_p , J	“White” layer thickness, μm	“White” layer microhardness, MPa	“White” layer continuity, %	Surface roughness, R_a , μm
Traditional CESA process (the first series)				
0.9	15–30	5347	50–60	0.8–0.9
2.6	30–60	9168	70–80	5.1–6.7
4.6	25–60	8492	70–80	8.3–9.0
Proposed CESA process (the second series)				
0.9	50–70	9932		0.9–1.0
2.6	80–100	10796	100	2.8–3.7
4.6	100–230	10796		3.2–4.8

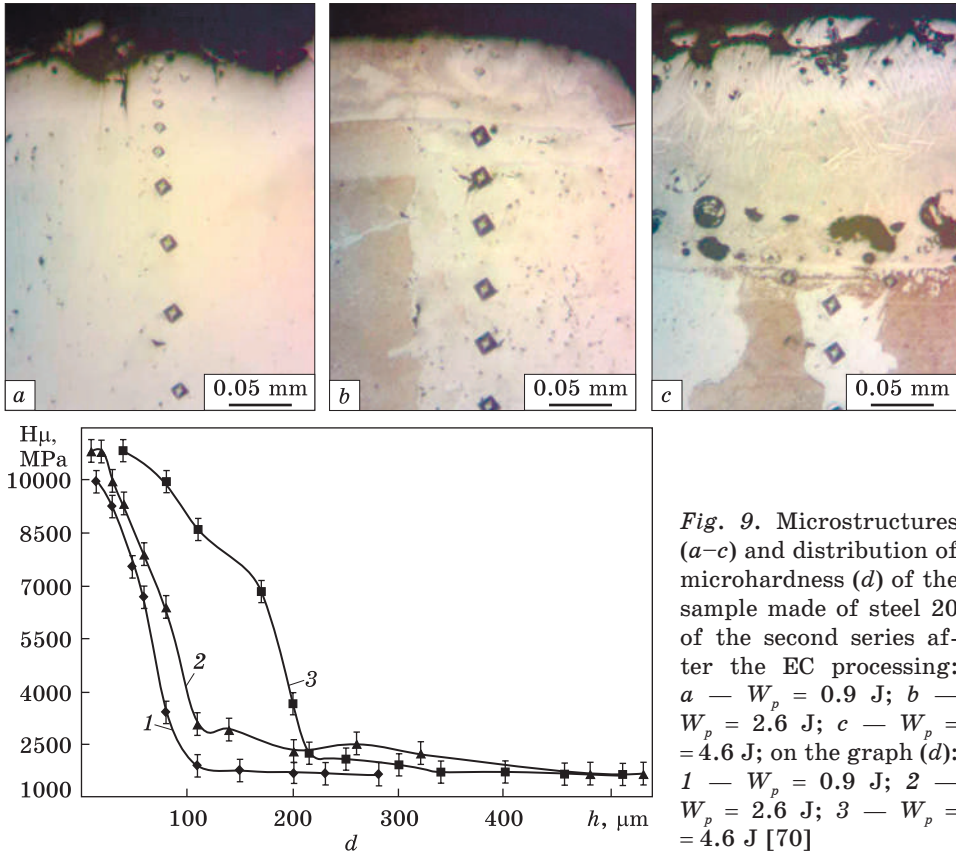


Fig. 9. Microstructures (a-c) and distribution of microhardness (d) of the sample made of steel 20 of the second series after the EC processing: a — $W_p = 0.9$ J; b — $W_p = 2.6$ J; c — $W_p = 4.6$ J; on the graph (d): 1 — $W_p = 0.9$ J; 2 — $W_p = 2.6$ J; 3 — $W_p = 4.6$ J [70]

From Ref. [67], it is known that when passing between the electrodes, a single electric pulse contributes to the formation of a pit with the edges slightly raised above the primary surface of the metal on the surface of the cathode (the sample). The size of the pit and the amount of the transferred material mainly depend on the erosion resistance of the electrode material and the energy of the single pulse.

Based on the above, it is possible to describe schematically, but with a high degree of probability, the process of forming the coating on the surface being treated in the course of processing by a spark electric discharge. Initially, the treated surface is covered with pits. In this case, each subsequent discharge will pass through the edge of the pit (the most protruding portion of the surface), as the contact area of the alloying electrode always exceeds the diameter of the formed pit. All the subsequent electrical pulses would fall on the already treated surfaces, causing much less splashing metal from the cathode.

The essence of the process does not change even when the anode material forms no coatings, for example, when the anode is graphite. In

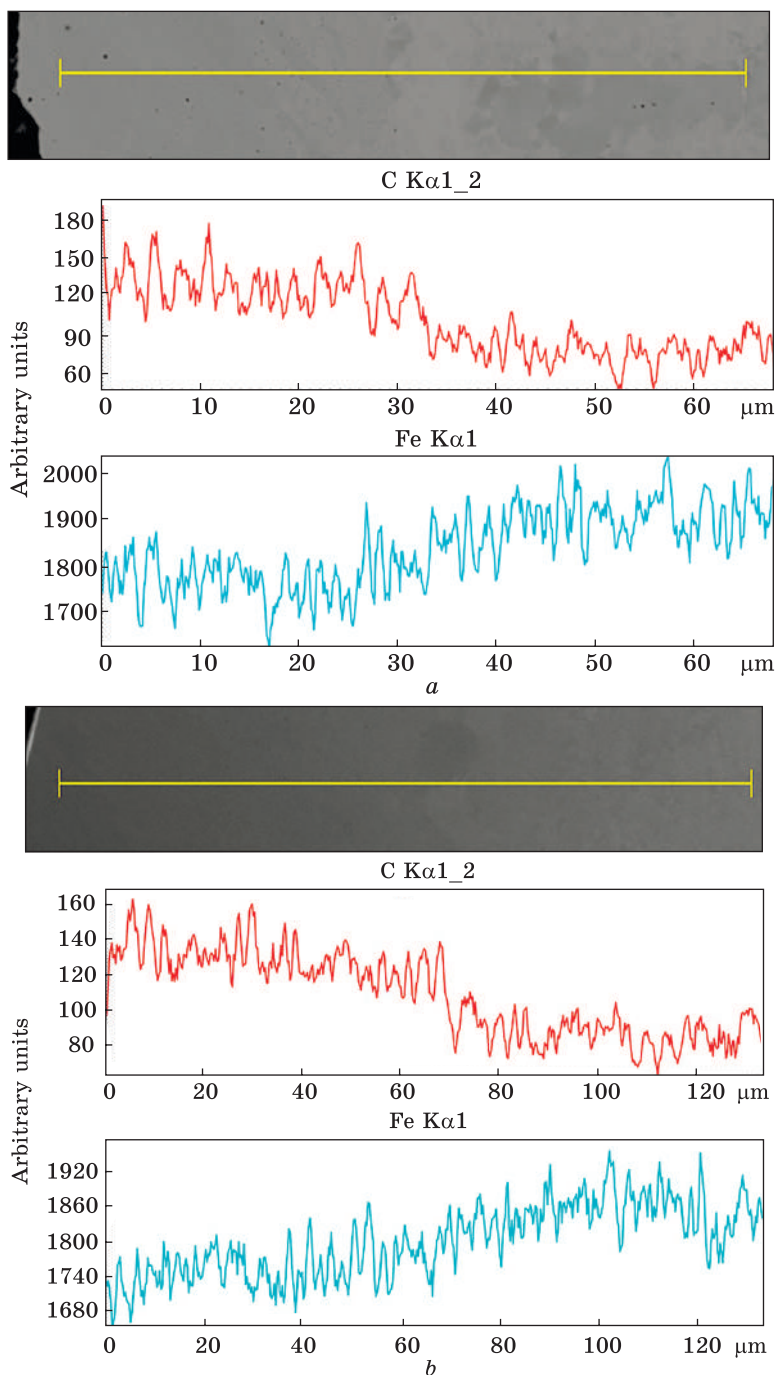


Fig. 10. The distribution of the elements in the surface layer of the samples made of steel 20 after the EC processing at discharge energy $W_p = 0.9$ J: a — the sample of the first series; b — the sample of the second series [70]

Table 6. Summary Table of surface quality parameters for the samples of steel 40X (40Kh) after the EC processing [70]

Discharge energy, W_p , J	“White” layer thickness, μm	“White” layer micro-hardness, MPa	“White” layer continuity, %	Surface roughness, R_a , μm
Traditional CESA process (the first series)				
0.9	25–40	5576–4243	50–60	0.9–1.1
2.6	40–70	8675–6538	70–80	5.4–6.3
4.6	55–80	8468–6976	70–80	8.5–9.2
Proposed CESA process (the second series)				
0.9	60–80	11351–7303		0.9–1.0
2.6	90–110	11787–6962	100	2.6–3.8
4.6	130–240	118239–7659		3.5–4.7

this case, the diffusion of materials is quite large and there is a significant change in the initial physicochemical properties of the surface being treated [67].

Thus, in the traditional method, when using any mode, at the beginning of the EC process on the surface of the sample (part) being treated, there is increased the roughness and each subsequent discharge passes through the most protruding portion of the surface, and the surface between the protrusions of the roughness is not alloyed with carbon. Hence, there occur low values of the continuity, the depth of diffusion of carbon, and the area of high hardness (Table 5).

Another picture is in the method proposed in paper [70]. At the second stage, the depressions between the protrusions of the roughness are filled with graphite powder, and at the third stage, the ESA process proceeds not only over the protrusions of the roughness, but also on the surface formed by the graphite powder, which increases the continuity of the alloyed layer up to 100% (Fig. 9). In addition, the repeated EC treatment at the third stage of the proposed technology results in saturating steel with carbon, increasing the depth of carbon diffusion as compared to traditional EC processing (Fig. 10), and in the condition of the accelerated procedure of cooling after EC processing, the “white” layer has a higher microhardness (9932 MPa), which is kept saved at a distance of up to 50–70 μm from the surface (Table 5).

When replacing the substrate material, steel 20 with steel 40X (40Kh), the quality of the surface layer does not change (Table 6). However, the microhardness of the “white” layer and its thickness increase.

Thus, the comparative analysis showed that after traditional EC processing at $W_p = 4.6$ J, the surface roughness is $R_a = 8.3–9.0$ μm , and after the proposed one, it is $R_a = 3.2–4.8$ μm . In this case, the continu-

ity of the alloyed layer is close to 100%, while the depth of the diffusion zone of carbon expands up to 80 μm , as well as the microhardness of the “white” layer and its thickness enhance up to 9932 MPa and up to 230 μm , respectively.

Nevertheless, it should be noted that the results obtained do not give a complete picture of the topography of the surface layer formed by the new EC technology, as well as the presence of crack pores, element composition, and other characteristic features of the structure.

Thus, a need arises to conduct the qualitative and quantitative elemental analyses of the surface layer formed with an increase in the contact area between the compact graphite tool electrode and the steel surface being strengthened, which is achieved owing to filling with graphite powder the roughness, pores and other defects formed when using the traditional technology for EC processing of the steel surfaces.

2.5. Electron Microscopic Studies of Coatings after EC Processing

In Ref. [69], topographic and qualitative x-ray microanalyses of the most characteristic areas of the steel sample surfaces after EC processing were carried out. The samples of steel 20 were used for the investigations (Table 7).

The two series of the samples were used for the research. In the first series, the samples were processed according to the traditional technology, namely, in the same mode and with the same productivity at EC processing by a compact tool electrode. In the second series, the samples were processed stepwise as described above. Both in the first and in the second series, the samples were processed at $W_p = 0.9, 2.6, \text{ and } 4.6 \text{ J}$.

The distribution of the elements in the surface layer was determined using a scanning electron microscope with a low vacuum chamber and with a REM-106 energy dispersive microanalysis system. The microscope is designed to study the surface relief of various objects in the solid phase and to determine the elemental composition of the objects by x-ray microanalysis by the energies of characteristic radiation quanta in two modes: high vacuum and low vacuum. The investigation of the objects in secondary electrons provided the topographic contrast, and that in reflected electrons did the elemental contrast. The XR-100FASTSDD Detector of Amptek (USA) production was installed on the measuring

Table 7. Chemical composition of steel 20 in accordance with the DSTU 7809 (State Standards of Ukraine) [71]

C	Si	Mn	P	S	Cr	Cu	Ni
0.17–0.24	0.17–0.37	0.35–0.65	≤ 0.035	≤ 0.04	≤ 0.25	≤ 0.3	≤ 0.3

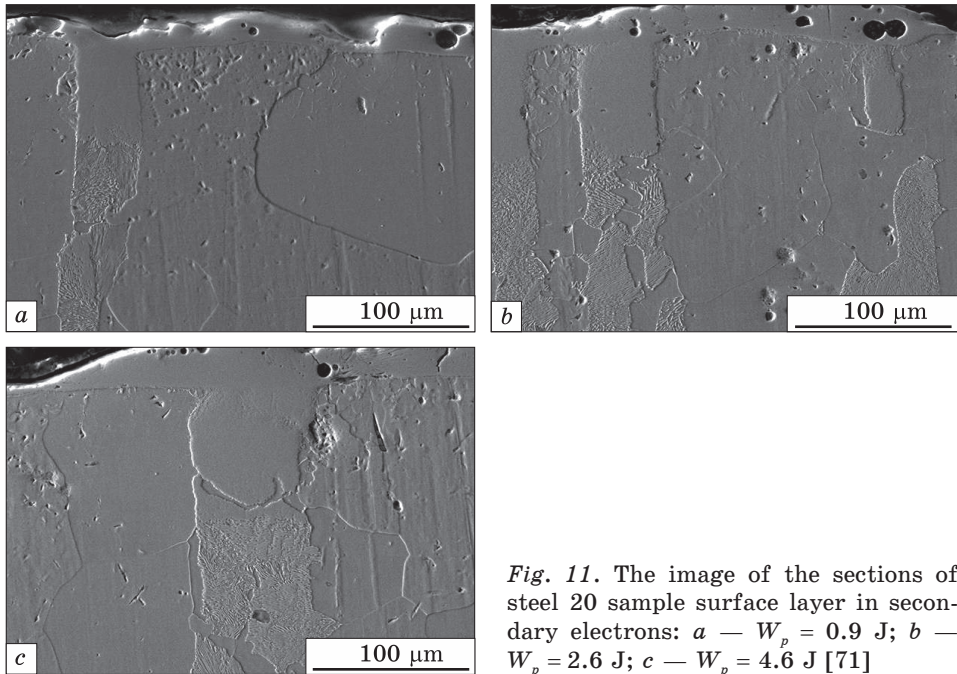


Fig. 11. The image of the sections of steel 20 sample surface layer in secondary electrons: *a* — $W_p = 0.9$ J; *b* — $W_p = 2.6$ J; *c* — $W_p = 4.6$ J [71]

instrument and allowed conducting the qualitative and quantitative elemental analyses of the area of the object under study.

As a result of the analysis of various sections of the surface layers from the set of the samples of the first series of steel 20, which were depicted in reflected and secondary electrons, it had been found that a layer of a changed structure was formed on the surface of the anode and cathode. This layer, when exposed to the etchants that were used to reveal the microstructure of electrode materials, remained “white”, namely, its structure could not be revealed. According to [70, 71], such layers were observed on the surfaces of materials subjected to grinding, turning, milling, electromechanical processing, processing by shot, on friction surfaces after exposure to highly concentrated energy fluxes. Common to all these cases was that the formation of “white” layers occurred in the conditions of local action of high temperatures and pressures. In terms of the intensity of the impact on the surface layer, the ESA process significantly differs from the processes listed above (shock wave pressure: 0.1 Pa; temperature $(5-40) \cdot 10^3$ °C). The high rate of heat removal leads to the fact that within the layer thickness of the order of several micrometers, the temperature rapidly drops to the values of melting temperatures and the corresponding phase transformations. In this regard, such events as crystallization, phase transformations, diffusion, and chemical interaction accompanying the ESA process

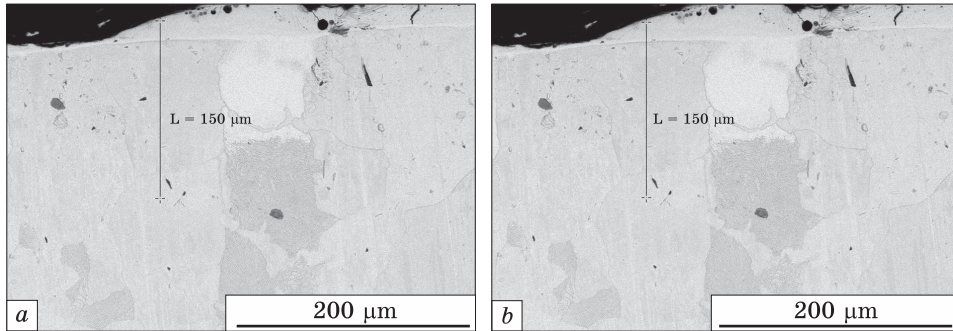


Fig. 12. The image of the sections of the samples of steel 20 surface layers in reflected electrons: *a* — for the first series; *b* — for the second series [71]

Table 8. Elemental composition of the coating on steel 20 at characteristic points of the first (*a*) and second (*b*) series of the samples after EC processing at the discharge energy of 4.6 J [71]

<i>a</i>						<i>b</i>					
Step	10	Time	60			Step	10	Time	60		
No.	C	Fe	Mn	Si	Σ	No.	C	Fe	Mn	Si	Σ
1	0.72	98.59	0.42	0.27	100	1	0.78	98.58	0.45	0.19	100
2	0.57	98.8	0.4	0.23	100	2	0.84	98.39	0.48	0.29	100
3	0.49	98.85	0.38	0.28	100	3	0.71	98.33	0.67	0.29	100
4	0.45	98.95	0.39	0.21	100	4	0.8	98.54	0.48	0.18	100
5	0.42	98.91	0.38	0.29	100	5	0.65	98.59	0.45	0.31	100
6	0.53	98.72	0.4	0.35	100	6	0.59	98.74	0.43	0.24	100
7	0.46	98.92	0.39	0.23	100	7	0.51	98.81	0.44	0.24	100
8	0.39	98.9	0.45	0.26	100	8	0.4	98.88	0.5	0.22	100
9	0.33	98.82	0.54	0.31	100	9	0.38	98.92	0.45	0.25	100
10	0.35	98.98	0.44	0.23	100	10	0.39	98.91	0.4	0.3	100
11	0.34	99.07	0.38	0.21	100	11	0.34	98.86	0.45	0.35	100
12	0.35	98.91	0.42	0.32	100	12	0.4	98.87	0.48	0.25	100
13	0.23	99.08	0.4	0.29	100	13	0.33	99.01	0.44	0.22	100
						14	0.38	98.86	0.49	0.27	100
						15	0.35	98.88	0.46	0.31	100
						16	0.25	99.06	0.41	0.28	100
						17	0.27	99.17	0.36	0.2	100
						18	0.17	99.24	0.36	0.23	100

lead to the formation of extremely nonequilibrium structures with very fine grains, high heterogeneity as for composition, structure, and properties. The hardness of such a layer, as a rule, significantly exceeds the hardness of the electrode materials. The stresses acting therein exceed the internal stresses in the electrode materials of the anode and cathode.

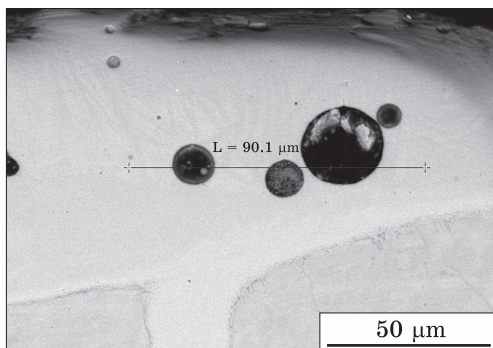


Fig. 13. The section of the surface layer of the steel 20 sample of the second series, EC processing at $W_p = 0.9$ J, the image is in reflected electrons [71]

The areas of the “white” layer depicted in the secondary electrons form a smooth surface. In the near-surface layer, there are individual cracks and pores sized from 1 to 5 microns. With increasing W_p , the depth of pore propagation increases from 3 to 7 μm (Fig. 11).

As a result of the studies carried out, it has been found that with an increase in W_p , the depth of the layer having an elevated concentration of carbon becomes larger, and is, respectively, 70, 100, and 120 μm . The amount of carbon, which is of 0.72 to 0.86% on the surface, and while deepening, the above said carbon amount is decreasing to a value corresponding to the carbon content in the base metal (0.17–0.24%).

Like for the samples of the first series, in the figures depicting the topographic contrast of the samples of the second series, the areas of the “white layer” form a smooth surface. A distinctive feature of steel 20 sample surface layer formed with the use of the new technology is the fact that there are significantly fewer pores in the near-surface layer, however, there are individual cracks ranging in size from 3 to 10 μm , the propagation depth of which increases with increasing discharge energy. In addition, with an increase in the discharge energy from 0.9 to 2.6 and 4.6 J, the depth of the layer, which has enlarged carbon con-

Table 9. Elemental composition of the coating at the characteristic points after EC processing at $W_p = 0.9$ J on the steel 20 samples of the second series [71]

Step	10	Time	60			Step	10	Time	60		
No.	C	Fe	Mn	Si	Σ	No.	C	Fe	Mn	Si	Σ
1	0.63	98.56	0.51	0.3	100	6	3.38	94.7	0.77	1.15	100
2	0.75	98.51	0.48	0.26	100	7	18.1	80.06	0.54	1.3	100
3	13.71	84.54	0.68	1.07	100	8	21.36	77.55	0.56	0.53	100
4	0.68	98.49	0.5	0.33	100	9	0.79	98.45	0.47	0.29	100
5	0.55	98.64	0.51	0.3	100	10	0.67	98.6	0.42	0.31	100

tent, is greater than in the first series of the samples, and, respectively, it is equal to 80, 120, and 170 μm . As the carbon deepens, its amount, which is of 0.75 to 0.84% on the surface, decreases to a value corresponding to its amount in the base metal of 0.17 to 0.24%.

In Fig. 12, there are shown the separate sections of the sample surface layers of the first (a) and second (b) series of the steel 20 samples obtained after EC processing at $W_p = 4.6$ J, which are depicted in reflected electrons, and here characterizing their elemental contrast, and also, there are shown the lines along which the analysis of chemical elements has been carried out. The analysis results are summarized in Table 8.

The most characteristic feature of the new EC technology is the provision of the presence of free graphite in the near-surface pores (Fig. 13) (Table 9), which can be used as a solid lubricant to improve the performance characteristics of the friction pair parts processed thereby.

Thus, as a result of the conducted studies of the steel 20 surface layers formed by the two methods, the traditional and proposed ones, it has been established as follows.

- With EC processing, which is carried out by the traditional way, the use of the values of W_p : 0.9, 2.6, and 4.6 J provides the formation of the surface layer with an increased carbon content in depth, respectively, 70, 100, and 120 μm , and by the proposed one, those values are 80, 120, and 170 μm . At the deepening, the content of carbon decreases from 0.72–0.86% to the amount thereof in the base metal: 0.17–0.24%.

- In the near-surface layer formed by the new technology, the pores are filled with free graphite, which can be used as a solid lubricant to improve the performance characteristics of the friction pair parts processed thereby.

Thus, the analysis of the literature data indicates the authors' interest in using graphite as an electrode material. However, it should be noted that, in general, the operational field of the application of the ESA method with a graphite electrode is limited to the tool-making facilities. In a number of works [21, 54, 70], the use of a graphite electrode in the EEA processes is associated with the study of the effect of energy parameters on structural changes in surface layers and is aimed at determining the overall diffusion coefficient. In some works, there is made mention of the use of the EEA method with a graphite electrode as an auxiliary operation aimed at reducing the roughness parameter of a previously processed surface.

4. Conclusions

The influence of the parameters of the electric-spark alloying process with a graphite electrode on the quality of the carburized layer has been investigated. The microstructural analysis showed that the three char-

acteristic zones could be distinguished in the structure: the carburized (“white”) layer, the finely dispersed transition zone with fine grain, and the base metal zone. The Vickers hardness on the surface is 1350 and 760 *HV* for 38XMIOA (38KhMYuA) and 40XH2MIOA (40KhN2MyuA) steels, respectively. While deepening, the hardness is decreasing and smoothly transforming into the hardness of the base, respectively, 225 and 250 *HV*. It has been set that in the course of carburizing steel surfaces by the electric-spark alloying method, with an increase in the discharge energy and the productivity (alloying time), not only the thickness of the strengthened layer increases, but also the surface roughness does. The phase analysis has showed that because of strengthening the 40X (40Kh) steel samples, the γ -Fe phase (25%) and iron carbide (Fe_3C) (63%) are formed, as a result of which the microhardness of the surface layer increases. In the coating on steel 30X13 (30Kh13), the formations of γ -Fe and the iron and chromium carbides, respectively, Fe_3C and Cr_{23}C_6 , are observed, and the formation of the carbides directly depends on the mode of the processing energy: the higher the mode, the greater the percentage of the carbide formation is available in the total phase composition of the surface strengthened layer; in the layer on steel 12X18H10T (12Kh18N10T), the following phases are formed: α -Fe, γ -Fe and X-phase. The X-phase is understood as a phase having an indefinite structural formula.

To achieve the required parameters of dimensional accuracy and roughness of the working surface of the part after the EC process, it is necessary to use additional processing methods. Such methods can be, for example, grinding with abrasive wheels and the methods of surface plastic deformation such as ball rolling, diamond burnishing, NAUF, *etc.* As a result of the surface plastic deformation methods applied after EC processing, the surface roughness decreases, the tensile stresses change to the compressive ones, and the fatigue strength increases by the value up to 20%.

The paper investigates the effect of the stepwise electrospark alloying method with graphite on the quality of the carburized layer. The ESA technology is proposed to be used for the surfaces after EC processing with the same graphite electrode, but in stages, while at each subsequent stage, the spark discharge energy should be reduced. This technology has proven to be effective. Therefore, after EC processing of 38XMIOA (38KhMYuA) steel at $W_p = 2.83$ J, the surface roughness is $R_a = 5.7\text{--}6.9$ μm . After EC processing with the productivity of $T = 2$ min/ cm^2 and at $W_p = 0.9$ J, the surface roughness is $R_a = 1.7\text{--}2.2$ μm . With the subsequent stepwise alloying process, there can be obtained $R_a = 1.1\text{--}1.2$ μm .

In order to increase the quality of the carburized layer obtained by the ESA method with a graphite electrode, it is proposed to use a graph-

ite powder, which is applied to the treated surface before alloying. The comparative analysis has shown that after the traditional EC process at $W_p = 4.6$ J, the surface roughness of steel 20 is $R_a = 8.3\text{--}9.0$ μm , and after the proposed technology, $R_a = 3.2\text{--}4.8$ μm . In this case, the continuity of the alloyed layer increases up to 100%, there increases the depth of the diffusion zone of carbon up to 80 μm , as well as the microhardness of the “white” layer and its thickness, up to 9932 MPa and up to 230 μm , respectively. As a result of research on an electron microscope, it has been established that at the EC process, which is carried out in the traditional way, the application of W_p : 0.9, 2.6, and 4.6 J provides the formation of a surface layer with a high carbon content depth, respectively, 70, 100, and 120 μm , and with the use of a graphite powder — 80, 120, and 170 μm . While deepening, the amount of carbon is decreasing from the values of 0.72 to 0.86% to the carbon content in the base metal that is, to the values of 0.17 to 0.24%. This is owing to the fact that in the near-surface layer formed by the new technology, the pores are filled with free graphite, which can be used as a solid lubricant to improve the performance of friction pairs parts processed thereby.

REFERENCES

1. I.P. Shatskyi, V.V. Perepichka, and L.Ya. Ropyak, *Metallofiz. Noveishie Tekhnol.*, **42**, No. 1: 69 (2020) (in Ukrainian);
<https://doi.org/10.15407/mfint.42.01.0069>
2. A. Umanskii, M. Storozhenko, I. Hussainova, A. Terentiev, A. Kovalchenko, and M. Antonov. *Powder Metall. Met. Ceram.*, **53**, Nos. 11–12: 663 (2015);
<https://doi.org/10.1007/s11106-015-9661-3>
3. O. Umanskyi, M. Storozhenko, M. Antonov, O. Terentyev, O. Koval, and D. Goljandin, *Key Engineering Materials*, **799**: 37 (2019);
<https://doi.org/10.4028/www.scientific.net/KEM.799.37>
4. M.S. Storozhenko, A.P. Umanskii, A.E. Terentiev, and I.M. Zakiev, *Powder Metall. Met. Ceram.* **56**, Nos. 1–2: 60 (2017);
<https://doi.org/10.1007/s11106-017-9872-x>
5. O. Umanskyi, M. Storozhenko, G. Baglyuk, O. Melnyk, V. Brazhevsky, O. Chernyshov, O. Terentiev, Yu. Gubin, O Kostenko, and I. Martsenyuk, *Powder Metall. Met. Ceram.* **59**, Nos. 7–8: 434 (2020);
<https://doi.org/10.1007/s11106-020-00177-y>
6. F.A.P. Fernandes, S.C. Heck, R.G. Pereira, A. Lombardi-Neto, G.E. Totten, and L.C. Casteletti, *Journal of Achievements in Materials and Manufacturing Engineering*, **40**, No. 2: 175 (2010).
7. S. Yeh, L. Chiu, and H. Chang, *Engineering*, **9**, No. 3: 942 (2011);
<https://doi.org/10.4236/eng.2011.39116>
8. S. Slima, *Materials Sciences and Applications*, **9**, No. 3: 640 (2012);
<https://doi.org/10.4236/msa.2012.39093>
9. L. Ropyak, I. Schuliar, and O. Bohachenko, *Eastern-European Journal of Enterprise Technologies*, **1**, No. 5 (79): 53 (2016) (in Ukrainian);
<https://doi.org/10.15587/1729-4061.2016.59850>

10. L.Ya. Ropyak, T.O. Pryhorovska, and K.H. Levchuk, *Prog. Phys. Met.*, **21**, No. 2: 274 (2020);
<https://doi.org/10.15407/ufm.21.02.274>
11. L.Ya. Ropyak, I.P. Shatskyi, and M.V. Makoviichuk, *Metallofiz. Noveishie Tekhnol.*, **41**, No. 5: 647 (2019) (in Ukrainian);
<https://doi.org/10.15407/mfint.41.05.0647>
12. V.I. Kuz'min, A.A. Mikhal'chenko, O.B. Kovalev, E.V. Kartaeu, and N.A. Rudenskaya, *Journal of Thermal Spray Technology*, **21**, No. 1: 159 (2012);
<https://doi.org/10.1007/s11666-011-9701-6>
13. A.D. Pogrebnyak, V.I. Ivashchenko, P.L. Skrynskyy, O.V. Bondar, P. Konarski, K. Zaleski, S. Jurga, and E. Coy, *Composites Part B: Engineering*, **142**: 85 (2018);
<https://doi.org/10.1016/j.compositesb.2018.01.004>
14. O. Maksakova, S. Simoës, A. Pogrebnyak, O. Bondar, Y. Kravchenko, V. Beresnev, and N. Erdybaeva, *Materials Characterization*, **140**: 189 (2018);
<https://doi.org/10.1016/j.matchar.2018.03.048>
15. A.D. Pogrebnyak, V.M. Beresnev, K.V. Smyrnova, Ya.O. Kravchenko, P.V. Zukowski, and G.G. Bondarenko, *Mater. Lett.*, **211**: 316 (2018);
<https://doi.org/10.1016/j.matlet.2017.09.121>
16. G. Morand, P. Chevallier, L. Bonilla-Gameros, Stéphane Turgeon, Maxime Cloutier, M. Da Silva Pires, A. Sarkissian, M. Tatoulian, L. Houssiau, and D. Mantovani, *Surface and Interface Analysis*, **53**, No. 7: 658 (2021);
<https://doi.org/10.1002/sia.6953>
17. G. Maistro, S. Kante, L. Nyborg, and Y. Cao, *Surfaces and Interfaces*, **24**: 101093 (2021); <https://doi.org/10.1016/j.surfin.2021.101093>
18. V.G. Smelov, A.V. Sotov, and S.A. Kosirev, *ARNP Journal of Engineering and Applied Sciences*, **9**, No. 10: 1854 (2014) (in Russian);
<https://doi.org/10.18287/2412-7329-2015-14-3-2-425-431>
19. B. Antoszewski and V. Tarel'nyk, *Appl. Mech. Mater.*, **630**: 301 (2014);
<https://doi.org/10.4028/www.scientific.net/AMM.630.301>
20. B. Antoszewski, S. Tofil, M. Scendo, and W. Tarelnik, *IOP Conf. Ser.: Mater. Sci. Eng.*, **233**: 012036 (2017);
<https://doi.org/10.1088/1757-899X/233/1/012036>
21. I. Pliszka and N. Radek, *Procedia Engineering*, **192**: 707 (2017);
<https://doi.org/10.1016/j.proeng.2017.06.122>
22. Y.K. Mashkov, D.N. Korotaev, M.Y. Baibaratskaya, and B.Sh. Alimbaeva, *Tech. Phys.*, **60**, No. 10: 1489 (2015);
<https://doi.org/10.1134/S1063784215100217>
23. V.B. Tarel'nyk, O.P. Gaponova, V.B. Loboda, E.V. Konoplyanchenko, V.S. Martsinkovskii, Yu.I. Semirnenko, N.V. Tarel'nyk, M.A. Mikulina, and B.A. Sarzhanov, *Surf. Engin. Appl. Electrochem.*, **57**, No. 3: 173 (2021);
<https://doi.org/10.3103/S1068375521020113>
24. V.B. Tarel'nyk, A.V. Paustovskii, Y.G. Tkachenko, V.S. Martsinkovskii, E.V. Konoplyanchenko, and K. Antoshevskii, *Surf. Engin. Appl. Electrochem.*, **53**, No. 3: 285 (2017); <https://doi.org/10.3103/S1068375517030140>
25. V.B. Tarel'nyk, O.P. Gaponova, I.V. Konoplianchenko, and M.Ya. Dovzhyk, *Metallofiz. Noveishie Tekhnol.*, **39**, No. 3: 363 (2017) (in Russian);
<https://doi.org/10.15407/mfint.39.03.0363>
26. V.B. Tarel'nyk, O.P. Gaponova, I.V. Konoplianchenko, V.A. Herasymenko, and N.S. Evtushenko, *Metallofiz. Noveishie Tekhnol.*, **40**, No. 2: 235 (2018) (in Russian);
<https://doi.org/10.15407/mfint.40.02.0235>

27. V.B. Tarelnyk, O.P. Gaponova, Ye.V. Konoplyanchenko, N.S. Yevtushenko, and V.O. Herasymenko, *Metallofiz. Noveishie Tekhnol.*, **40**, No. 6: 795 (2018) (in Russian); <https://doi.org/10.15407/mfint.40.06.0795>
28. V.B. Tarelnyk, A.V. Paustovskii, Y.G. Tkachenko, E.V. Konoplianchenko, V.S. Martsynkovskyy, and B. Antoszewski, *Powder Metall. Met. Ceram.*, **55**: Nos. 9–10: 585 (2017); <https://doi.org/10.1007/s11106-017-9843-2>
29. V. Tarelnyk, V. Martsynkovskyy, O. Gaponova, Ie. Konoplianchenko, M. Dovzyk, N. Tarelnyk, and S. Gorovoy, *IOP Conf. Ser.: Mater. Sci. Eng.*, **233**: 012049 (2017); <https://doi.org/10.1088/1757-899X/233/1/012049>
30. D.N. Korotaev, *Tekhnologicheskie Vozmozhnosti Formirovaniya Iznosostoikikh Nanostruktur Ehlektroiskrovym Legirovaniem* [Technological Possibilities of Wear-Resistant Nanostructure Formation by Electric-Spark Alloying], (Omsk: SibADI: 2009) (in Russian).
31. A.D. Verkhoturov, *Formirovanie Poverkhnostnogo Sloya Metallov pri Ehlektroiskrovom Legirovanii* [Formation of the Metal Surface Layer by Electric-Spark Alloying], (Vladivostok: Dal'nauka: 1995) (in Russian).
32. A.I. Mikhailyuk and A.E. Gitlevich, *Surf. Engin. Appl. Electrochem.*, **46**, No. 5: 424 (2010); <https://doi.org/10.3103/S1068375510050054>
33. Yusuf Kayali and Şükrü Talaş, *Prot. Met. Phys. Chem. Surf.*, **57**, No. 1: 106 (2021); <https://doi.org/10.1134/S2070205120060131>
34. Y.G. Tkachenko, O.I. Tolochyn, V.F. Britun, and D.Z. Yurchenko, *Powder Metall. Met. Ceram.*, **58**, Nos. 11–12: 692 (2020); <https://doi.org/10.1007/s11106-020-00126-9>
35. N. Radek, J. Pietraszek, and A. Szczotok, *Int. Conf. on Metallurgy and Materials, METAL 2017 (May 24–26, 2017, Brno)* (Ostrava: 2018), p. 1432.
36. A.E. Gitlevich, V.V. Mikhailov, N.Ya. Parkanskii, and V.M. Revutskii, *Ehlektroiskrovoe Legirovanie Metallicheskih Poverkhnostei* [Electrospark Alloying of Metal Surfaces] (Chisinau: Shtiintsa: 1985) (in Russian).
37. V.S. Martsynkovskyy, V.B. Tarelnyk, and A.B. Belous, *Sposib Tsementatsii Stalevykh Detalei Ehlektroeroziinym Leguvanniam* [Method of Cementation of Steel Parts by Electroerosion Alloying], Patent 82948 UA. MKI (2006), C23C 8/00 (Publ. Bul. No. 10: 3) (2008) (in Ukrainian).
38. V.S. Martsynkovskyy, V.B. Tarelnyk, and M.P. Bratushchak, *Sposib Tsementatsii Stalevykh Detalei Ehlektroeroziinym Leguvanniam* [Method of Cementation of Steel Parts by Electroerosion Alloying], Patent 101715 UA. MKI (2013.01), B23H 9/00, (Publ. Bul. No. 8: 7) (2013) (in Ukrainian).
39. V.B. Tarelnyk, V.S. Martsynkovskyy, O.P. Gaponova, O.M. Myslyvchenko, V.O. Pirogov, O.O. Gapon, and A.D. Lazarenko, *Sposib Tsementatsii Stalevykh Detalei Ehlektroeroziinym Leguvanniam* [Method of Cementation of Steel Parts by Electroerosion Alloying], Patent 142822 UA. MKI (2020.01), C23C 8/00, C23C 28/00, (Publ. Bul. No. 12: 8) (2020) (in Ukrainian).
40. V.B. Tarelnyk, V.S. Martsynkovskyy, O. A. Sarzhanov, O.O. Gapon, B.O. Sarzhanov, O.P. Gaponova, and E.V. Konoplyanchenko, *Sposib Ehkologichno Bezpechnogo Zmitsnennia Detalei z Lystovoi Stali Metodod Ehlektroeroziinogo Leguvannia Stalevykh Poverkhon Grafitovym Ehlektrodom* [A Method of Environmentally Friendly Hardening of Sheet Steel Parts by Electroerosion Alloying

- of Steel Surfaces with a Graphite Electrode], Patent 141992 UA. MKI (2020.01) B23P 6/00, B23K 9/04 (2006.01), B23H 5/00, B23H 5/02 (2006.01), (Publ. Bul. No. 9: 9) (2020) (in Ukrainian).
41. V.B. Tarel'nik, A.V. Paustovskii, Yu.G. Tkachenko, V.S. Martsinkovskii, A.V. Belous, E.V. Konoplyanchenko, and O.P. Gaponova, *Surf. Engin. Appl. Electrochem.*, **54**, No. 2: 147 (2018);
<https://doi.org/10.3103/S106837551802014X>
 42. V.B. Tarel'nyk, O.P. Gaponova, Ye.V. Konoplianchenko, V.S. Martsynkovskyy, N.V. Tarel'nyk, and O.O. Vasylenko, *Metallofiz. Noveishie Tekhnol.*, **41**, No. 1: 47 (2019);
<https://doi.org/10.15407/mfint.41.01.0047>
 43. V.B. Tarel'nik, E.V. Konoplyanchenko, P.V. Kosenko, and V.S. Martsinkovskii, *Chem. Petrol. Eng.*, **53**, Nos. 7–8: 540 (2017);
<https://doi.org/10.1007/s10556-017-0378-7>
 44. V.B. Tarel'nik, V.S. Martsinkovskii, and A.N. Zhukov, *Chem. Petrol. Eng.* **53**, Nos. 3–4: 266 (2017);
<https://doi.org/10.1007/s10556-017-0333-7>
 45. V.B. Tarel'nik, V.S. Martsinkovskii, and A.N. Zhukov, *Chem. Petrol. Eng.* **53**, Nos. 5–6: 385 (2017);
<https://doi.org/10.1007/s10556-017-0351-5>
 46. A.I. Mikhaylyuk, *Ehlektronnaya Obrabotka Materialov* [Electronic Processing of Materials], **39**, No. 3: 21 (2003) (in Russian).
 47. V. Tarel'nyk, V. Martsynkovskyy, and A. Dziuba, *Appl. Mech. Mater.*, **630**: 388 (2014);
<https://doi.org/10.4028/www.scientific.net/AMM.630.388>
 48. V.B. Tarel'nyk and V.S. Martsynkovskyy, *Sposib Obrobky Spoluchnykh Poverkhon Detalei (Varianty)* [A method of Processing Connecting Surfaces of Details (Options)], Patent 66105 UA. MKI (2006), B23H 1/00, B23H 5/00, B23H 9/00, (Publ. Bul. No. 7: 3) (2008) (in Ukrainian).
 49. V.B. Tarel'nik, V.S. Martsinkovskii, and V.I. Yurko, *Chem. Petrol. Eng.*, **51**, Nos. 5–6: 328 (2015);
<https://doi.org/10.1007/s10556-015-0047-7>
 50. V. Martsinkovsky, V. Yurko, V. Tarel'nik, and Y. Filonenko, *Procedia Eng.*, **39**: 157 (2012);
<https://doi.org/10.1016/j.proeng.2012.07.020>
 51. V.B. Tarel'nik, V.S. Martsinkovskii, and A.N. Zhukov, *Chem. Petrol. Eng.* **53**, Nos. 1–2: 114 (2017);
<https://doi.org/10.1007/s10556-017-0305-y>
 52. V.B. Tarel'nik and A.V. Bilous, *Bulletin of Sumy National Agrarian University*, **11**: 115 (2005) (in Russian).
 53. A.V. Bilous, *Bulletin of Sumy National Agrarian University*, **12**: 158 (2006) (in Russian).
 54. V.B. Tarel'nik, B. Antoshevsky, V.S. Martsinkovsky, E.V. Konoplyanchenko, and A.V. Belous *Tsementatsiya Ehlektroehroziionnym Legirovaniem: Monografiya* [Cementation by Electroerosive Alloying: A Monograph] (Ed. V.B. Tarel'nik) (Sumy: University Book: 2015) (in Russian).
 55. A.I. Mikhaylyuk, A.Ye. Gitlevich, A.I. Ivanov, Ye.I. Fomicheva, G.I. Dimitrova, and A.N. Gripachevskiy, *Electronic Processing of Materials*, **4**: 23 (1986) (in Russian).
 56. V.M. Ershov, *Collection of Scientific Works of the Donbass State Technical University Staff*, **31**: 219 (2011) (in Russian).

57. A.I. Mikhailyuk, V.G. Revenko, and N.N. Natarov, *Physics and Chemistry of Materials Processing*, **1**: 101 (1993) (in Russian).
58. V.B. Tarelnik and A.V. Belous, *Compressor and Power Engineering*, **11**, No. 1: 90 (2008) (in Russian).
59. A.I. Mikhailyuk, L.S. Rapoport, and A.E. Gitlevich, *Electronic Processing of Materials*, **1**: 16 (1991) (in Russian).
60. A.I. Mikhailyuk, L.S. Rapoport, and A.E. Gitlevich, *Electronic Processing of Materials*, **2**: 17 (1991) (in Russian).
61. V.K. Yatsenko, G.Z. Zaitsev, and V.F. Pritchenko, *Povyshenie Nesushchey Spособnosti Detaley Mashin Almaznym Vyglazhivaniem* [Increasing the Bearing Capacity of Machine Parts by Diamond Burnishing] (Moscow: Mashinostroenie: 1985) (in Russian).
62. V.K. Yatsenko, V.F. Pritchenko, I.N. Komarchuk, and A.G. Sakhno, *Problems of Strength*, **5**: 119 (1987) (in Russian).
63. Yu.V. Kholopov, A.G. Zinchenko, and A.A. Savinykh, *Bezabrazivnaya Ultrazvukovaya Finishnaya Obrabotka Metallov* [Abrasive Ultrasonic Finishing of Metals] (Leningrad: LDNTP: 1988) (in Russian).
64. V.B. Tarelnik, V.S. Martsinkovskiy, and B. Antoshevskiy, *Povyshenie Kachestva Podshipnikov Skolzheniya: Monografiya* [Improving the Quality of Sliding Bearings: A Monograph] (Sumy: McDen Publishing House: 2006) (in Russian).
65. V.B. Tarelnik, *Kombinirovannye Tekhnologii Ehlektroerozionnogo Legirovaniya* [Combined Technologies of Electroerosive Alloying] (Kyiv: Tekhnika: 1997) (in Russian).
66. D.N. Garkunov, *Tribotekhnika* [Tribotechnology] (Moscow: Mashinostroenie: 1989) (in Russian).
67. N.I. Lazarenko, *Ehlektroiskrovoe Legirovanie Metallicheskih Poverkhnostey* [Electrospark Alloying of Metal Surfaces] (Moscow: Mashinostroenie: 1976) (in Russian).
68. V.B. Tarelnik, V.S. Martsinkovskiy, and B. Antoshevskiy, *Suchasni Metody Formuvorenniya Poverkhon Tertya Detaley Mashyn: Monografiya* [Modern Methods of Forming the Friction Surfaces of Machine Parts: A Monograph]. (Sumy: McDen Publishing House: 2012) (in Ukrainian).
69. O.V. Sizova and E.A. Kolubaev, *Izvestiya Vuzov. Fizika*, **2**: 27 (2003) (in Russian).
70. V.B. Tarelnyk, O.P. Gaponova, G.V. Kirik, Ye.V. Konoplianchenko, N.V. Tarelnyk, and M.O. Mikulina, *Metallofiz. Noveishie Tekhnol.*, **42**, No. 5: 655 (2020) (in Ukrainian);
<https://doi.org/10.15407/mfint.42.05.0655>
71. V. Tarelnyk, O. Gaponova, V. Martsynkovskyy, Ie. Konoplianchenko, V. Melnyk, V. Vlasovets, A. Sarzhanov, N. Tarelnyk, Du Xin, Yu. Semirnenko, S. Semirnenko, T. Voloshko, and O. Semernya, *2020 IEEE 10th International Conference Nanomaterials: Applications & Properties (NAP) (November 9–13, 2020, Sumy)* (IEEE Xplore: 2021), p. 01TFC13;
<https://doi.org/10.1109/NAP51477.2020.9309618>
72. A.D. Verkhoturov and I.M. Mukha, *Tekhnologiya Ehlektroiskrovogo Legirovaniya Metallicheskih Poverkhnostey* [Technology of Electrospark Alloying of Metal Surfaces] (Kyiv: Tekhnika: 1982) (in Russian).

Received 27.09.2021;
in final version, 19.01.2022

В.Б. Тарельник¹, О.П. Гапонова², Є.В. Коноплянченко¹

¹ Сумський національний аграрний університет,
вул. Герасима Кондратьєва, 160, 40021 Суми, Україна

² Сумський державний університет,
вул. Римського-Корсакова, 2, 40007 Суми, Україна

ЕЛЕКТРОІСКРОВОЕ ЛЕГУВАННЯ МЕТАЛЕВИХ ПОВЕРХОНЬ ГРАФІТОМ

Оглянуто та проаналізовано актуальні на сьогоднішній день наукові дослідження в області поверхневого оброблення металевих поверхонь концентрованими потоками енергії (КПЕ) — електроіскрового легування (ЕІЛ), яке уможливило одержання поверхневих структур з унікальними фізико-механічними та трибологічними властивостями на нанорівні. Досліджено вплив параметрів ЕІЛ графітовою електродою (електроіскрова цементация — ЕЦ) на якість цементованого шару. Мікроструктурна аналіза показала, що в структурі можна виділити три характерні зони: цементовий («білий») шар, перехідну зону з дрібнодисперсним зерном і зону основного металу. Встановлено, що із ЕЦ зі збільшенням енергії розряду та часу легування збільшується не лише товщина зміцненого шару, а й шерсткість поверхні. Задля досягнення необхідних параметрів розмірів і шерсткості робочої поверхні деталі після ЕЦ необхідне застосування методу безабразивного ультразвукового фінішного оброблення (БУФО). Крім цього, в результаті застосування БУФО знижується шерсткість поверхні, залишкові напруги змінюються з розтягувальних на стискальні, збільшується втомна міцність деталі. Також для зниження шерсткості оброблюваної поверхні запропоновано технологію ЕЦ застосовувати поетапно, знижуючи на кожному наступному етапі енергію іскрового розряду. З метою підвищення параметрів якості поверхневого шару, одержаного ЕЦ, запропоновано використовувати порошок графіту, який наноситься на оброблювану поверхню перед легуванням. При цьому до 100% збільшується суцільність легованого шару, до 80 мкм підвищується глибина дифузійної зони вуглецю, до 9932 МПа і до 230 мкм зростають мікротвердість «білого» шару та його товщина відповідно. Локальна мікрорентгеноспектральна аналіза одержаних покриттів показала, що при ЕЦ традиційним способом з енергією розряду у 0,9, 2,6 і 4,6 Дж забезпечується формування поверхневого шару з підвищеним вмістом Карбону глибиною 70, 100 і 120 мкм відповідно, а з використанням порошку графіту — 80, 120 і 170 мкм. Вміст Карбону у 0,72–0,86% по мірі заглиблення знижується до вмісту в основному металі — 0,17–0,24%. В приповерхневому шарі, сформованому за новою технологією, пори заповнені вільним графітом, який може бути використаний в якості твердого змащення для поліпшення експлуатаційних характеристик деталей пар тертя.

Ключові слова: електроіскрове легування, графіт, цементация, мікроструктура, якість, зносостійкість.